PENNSTATE

High-Power Considerations in Metamaterial Antennas

July 8, 2014

Jeremy A. Bossard, Clinton P. Scarborough*, Qi Wu, Douglas H. Werner, and Ping L. Werner

Department of Electrical Engineering
The Pennsylvania State University

Scott F. Griffiths

Joint Non-Lethal Weapons Directorate

REPORT DOCUMENTATION PAGE

Form Approved
OMB No. 0704-0188

1. REPORT DATE *(DD-MM-YYYY)*	**2. REPORT TYPE**	**3. DATES COVERED** *(From - To)*
25-06-2014	Brief	15-08-2012 to 25-06-2014

4. TITLE AND SUBTITLE

High-Power Considerations in Metamaterial Antennas

5a. CONTRACT NUMBER

5b. GRANT NUMBER

5c. PROGRAM ELEMENT NUMBER

6. AUTHOR(S)

Jeremy A. Bossard, Clinton P. Scarborough, Qi Wu, Douglas H. Werner, Ping L. Werner, Scott Griffiths

5d. PROJECT NUMBER

5e. TASK NUMBER

5f. WORK UNIT NUMBER

7. PERFORMING ORGANIZATION NAME(S) AND ADDRESS(ES)

Department of Electrical Engineering
The Pennsylvania State University
University Park, PA 16802 USA

8. PERFORMING ORGANIZATION REPORT NUMBER

9. SPONSORING / MONITORING AGENCY NAME(S) AND ADDRESS(ES)

Joint Non-Lethal Weapons Directorate
3097 Range Road
Quantico, VA 22134-5100

10. SPONSOR/MONITOR'S ACRONYM(S)
JNLWD

11. SPONSOR/MONITOR'S REPORT NUMBER(S)
JNLW14-020

12. DISTRIBUTION / AVAILABILITY STATEMENT
Statement A: Approved for Public Release; Distribution is unlimited.

13. SUPPLEMENTARY NOTES

14. ABSTRACT

Many metamaterial types rely on resonant behaviors that produce high fields within their structures.
However, if a metamaterial can operate away from resonance (e.g., low-index or zero-index metamaterials), it can be well-suited for HPM applications.
Artificial Magnetic Conducting surfaces often exhibit high field enhancement at resonance with unoptomized MFEFs over 30.
Genetic algorithm optimization was successfully employed to design single- and dual-band AMC surfaces with 50% reduced MFEF for HPM applications.

15. SUBJECT TERMS
Non-lethal weapons; low-index metamaterials; zero-index metamaterials; high-power; maximum field enhancement factor

16. SECURITY CLASSIFICATION OF:			**17. LIMITATION OF ABSTRACT**	**18. NUMBER OF PAGES**	**19a. NAME OF RESPONSIBLE PERSON**
Unclassified					Scott Griffiths
a. REPORT	**b. ABSTRACT**	**c. THIS PAGE**	SAR	24	**19b. TELEPHONE NUMBER** *(include area code)*
Unclassified	Unclassified	Unclassified			(703) 432-0909

PENNSTATE

Overview

1. Frequency Selective Surfaces and Metamaterials under High-Power Microwaves
2. Artificial Magnetic Conducting Surfaces
3. Periodic FE-BI Analysis
4. AMC Synthesis using Genetic Algorithms
5. Design of Single-Band and Dual-Band AMC Surfaces
6. Summary & Conclusion

Frequency Selective Surfaces for High-Power Microwave (HPM) Applications

Second-order Bandpass Filter with Low-profile Frequency Selective Surfaces (FSS)

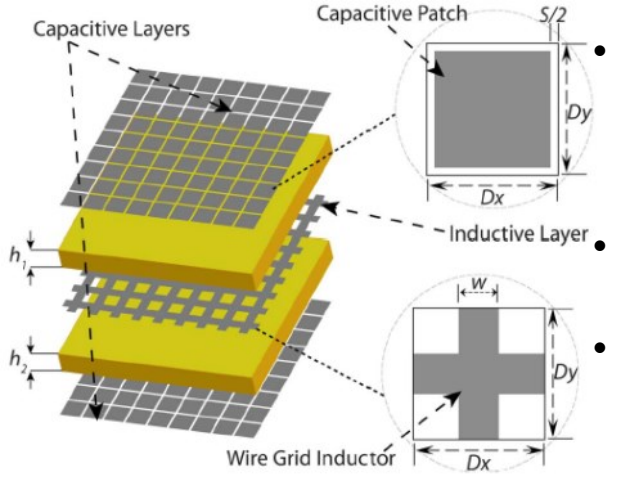

- Multi-layer FSS with non-resonant constitutive elements (metallic patches and wire grids).
- Verified filtering properties by HFSS simulations.
- Identified maximum electric field in the gap regions between capacitive patches.

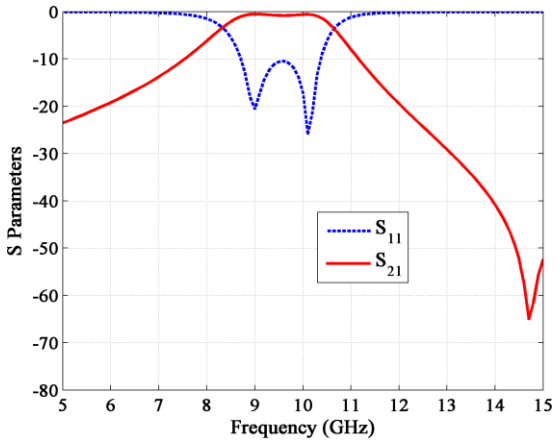

M. Al-Joumayly, and N. Behdad, "A New Technique for Design of Low-Profile, Second-Order, Bandpass Frequency Selective Surfaces," *IEEE Transactions on Antennas and Propagation*, Vol. 57, pp. 452-459, 2009.

Evaluated the electric field distributions on the top capacitive patch surface at different frequencies.

- Implemented numerical models based on full-wave simulations to effectively evaluate the electric field distributions within the metamaterial and FSS.
- The simulation results can be used to determine the power handling capability of such structures.

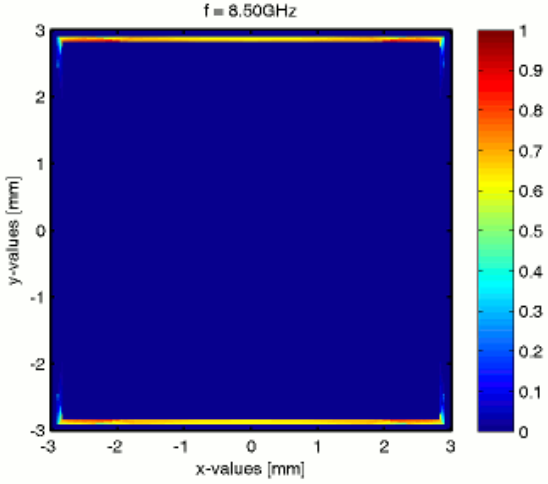

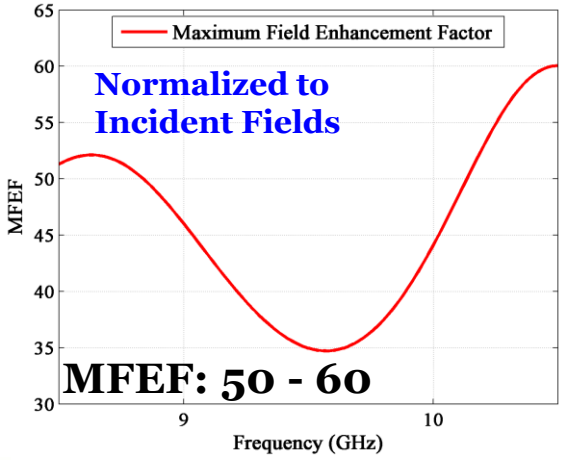

Frequency Selective Surfaces for High-Power Microwave (HPM) Applications

- Replacing the capacitive patches with high permittivity (*e.g.* ϵ_r=20) dielectric layers can reduce the maximum electric field enhancement factor.
- Peak power of 25 kW (power density of 1.08×10^8 W/m^2) was experimentally demonstrated.
- Both the filtering performance and field enhancement factor were verified by our full-wave numerical simulations.

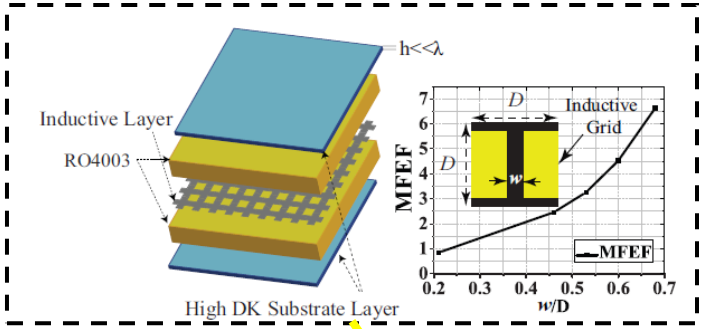

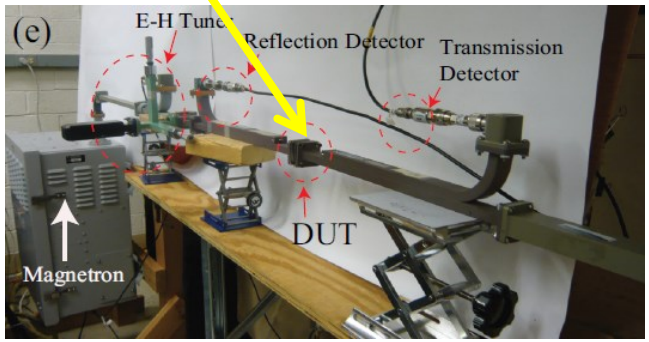

L. Meng, and N. Behdad, "Frequency Selective Surfaces for High-Power Microwave (HPM) Applications," *IEEE AP-S*, 2012.

Bandpass Filter with FSS

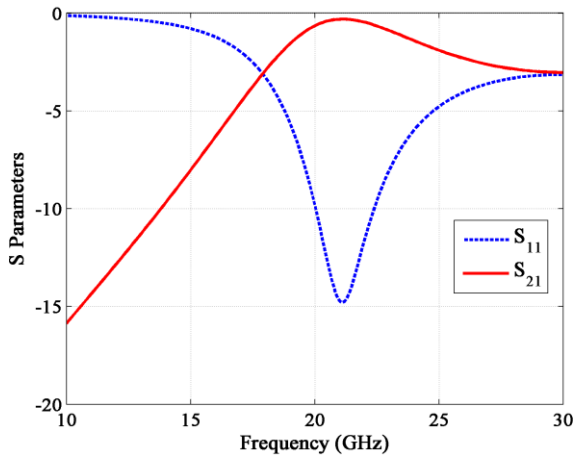

Maximum Field Enhancement Factor

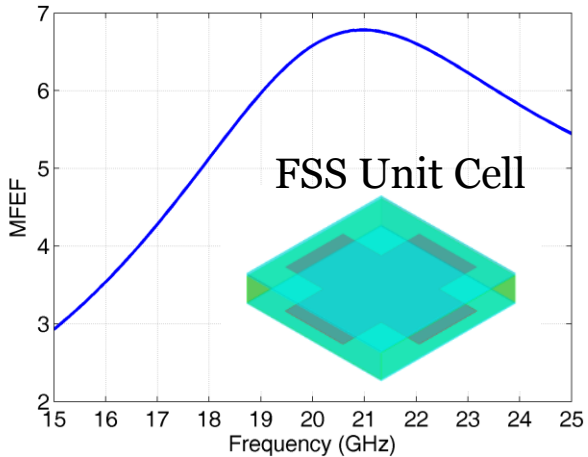

Electric Field Distributions on the Inductive Patch Surface

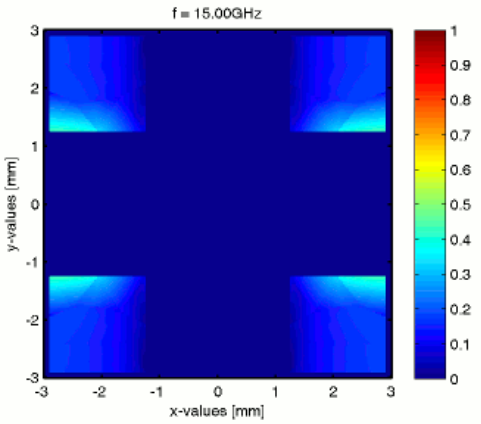

Metamaterials for High-power RF Applications

- Metamaterials with unit cells that support a confined resonance can have significantly stronger electric fields than the incident wave, which can cause voltage breakdown in air or dielectrics.
- HPM electromagnetic fields can induce losses and heating on the unit cells of metamaterials, which cause melting, structural deformation and variation in the responses.

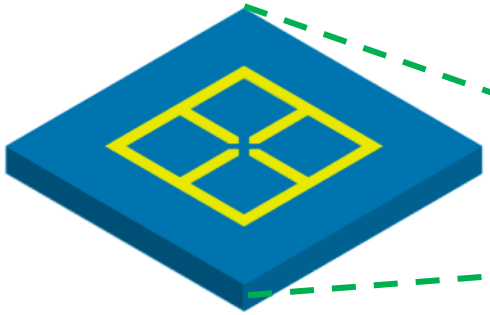

An electric LC resonator metamaterial unit cell composed of metallic traces on top of a dielectric substrate.

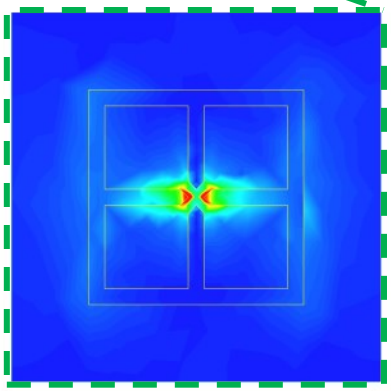

Maximum Field Enhancement Factor of 90 at 14.6 GHz

The metamaterial supports a strong LC resonance due to the gap capacitance and loop inductance, which gives rise to highly enhanced electric fields in the middle of the unit cell.

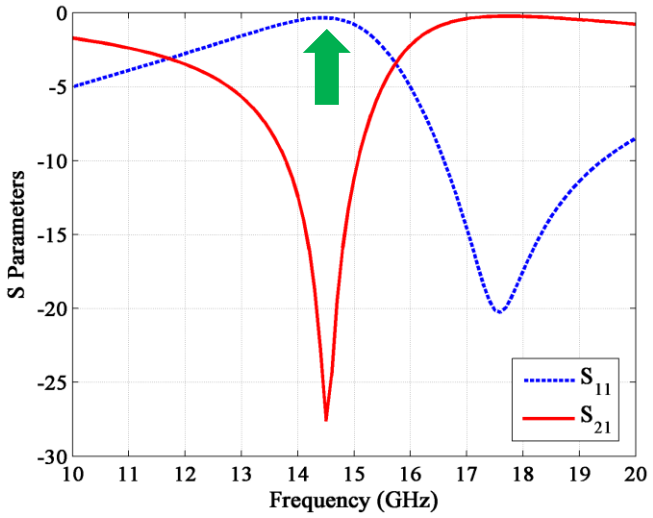

High-power Considerations for Negative Index Metamaterials

- A representative metamaterial, the negative index material (NIM), has been used to implement flat lenses with advanced focusing properties.
- Typical NIM designs exhibit high absorption losses and high field enhancement near the resonance, limiting their application for HPM.

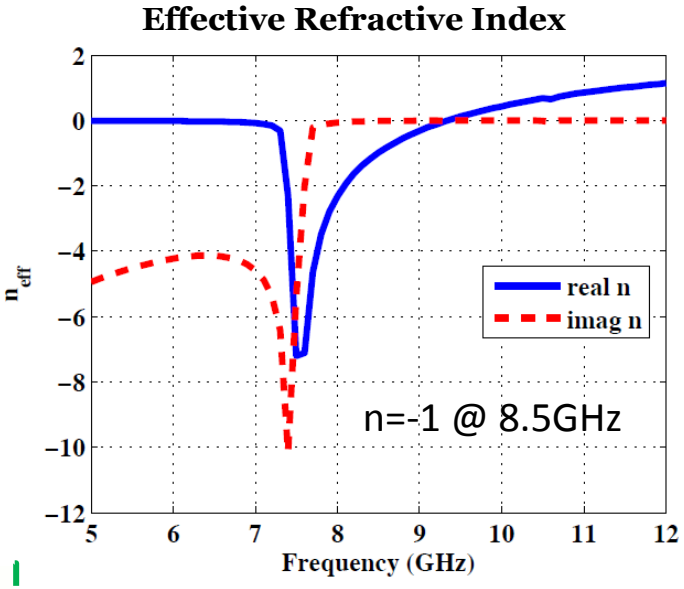

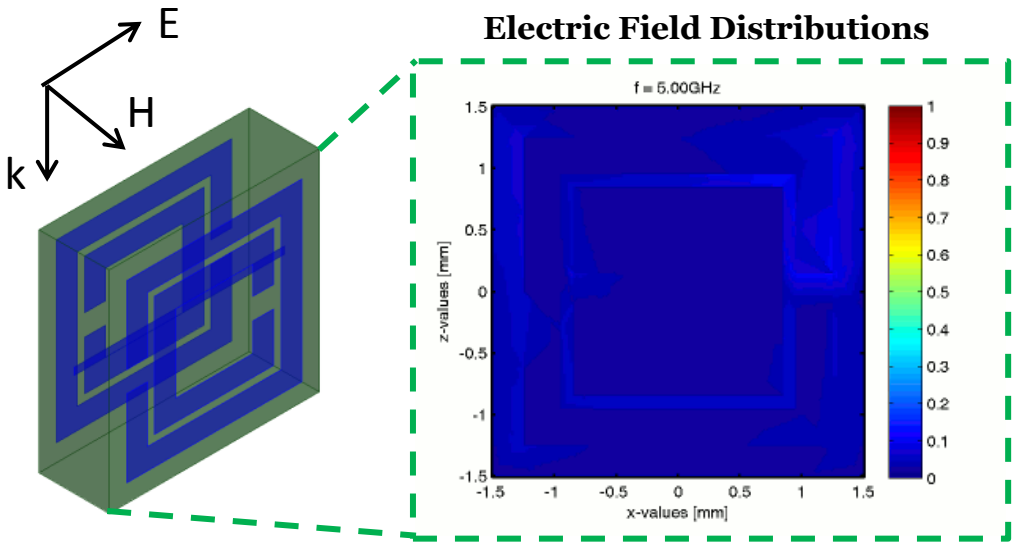

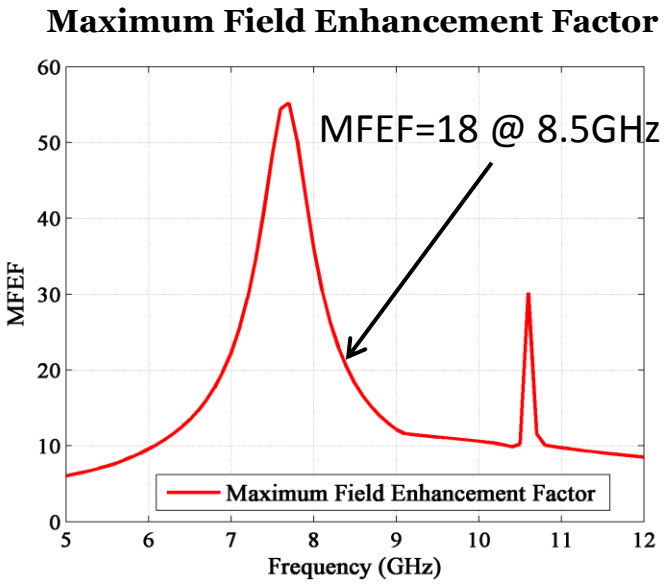

A negative index material composed of split ring resonators and metallic strips. The maximum field occurs at the surface of the split ring resonators.

Low Loss Negative Index Materials for High-power RF Applications

A negative index metamaterial design with low loss was realized by using powerful global optimization techniques.

Copper Layers
Thickness = 0.035mm

Rogers TMM4
ϵ_r=4.5; tanδ=0.002

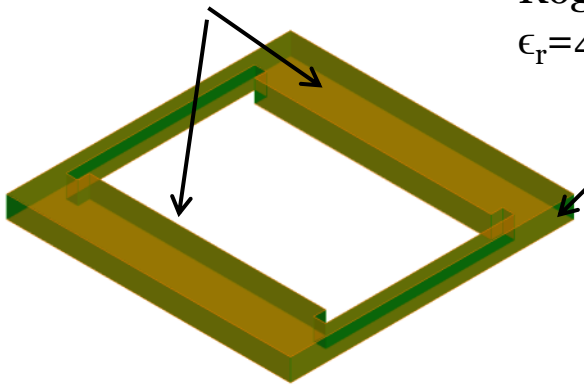

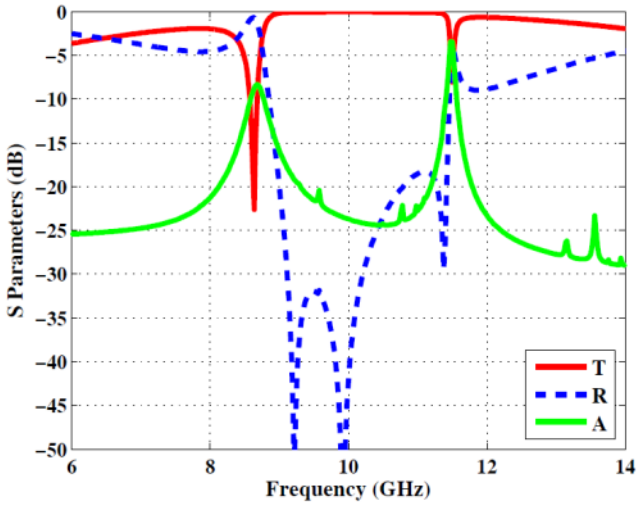

Achieved reduced absorption and reflection loss by optimizing the NIM structures.

Modified Fishnet with Notches

Effective Refractive Index

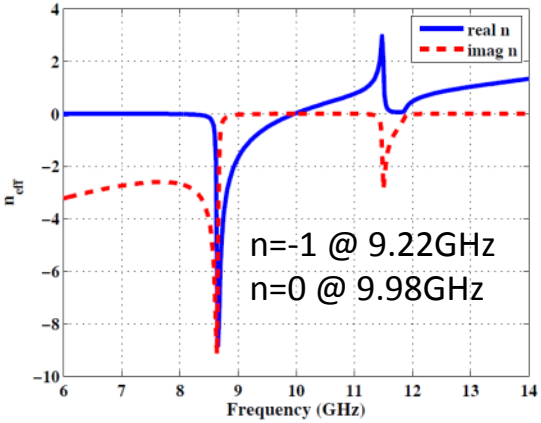

Effective Impedance

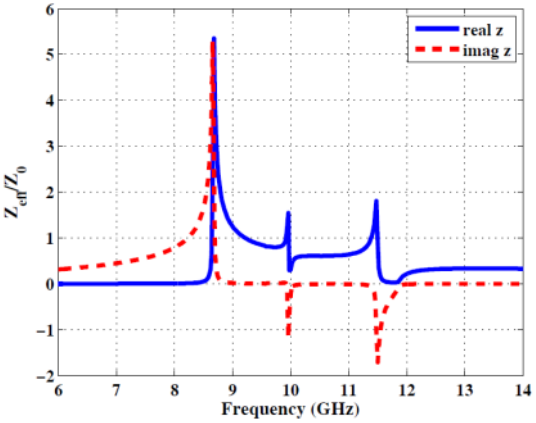

Z. Jiang, J. A. Bossard, and D. H. Werner, "Low Loss RF Modified Fishnet Metamaterials with Optimized Negative, Zero and Unity Refractive Index Behavior," *IEEE International Symposium on Antennas and Propagation and USNC/URSI National Radio Science Meeting*, 2009.

Low Loss Negative Index Materials for High-power RF Applications

Maximum *E* field occurs at the top metallic patch layer (blue curve)

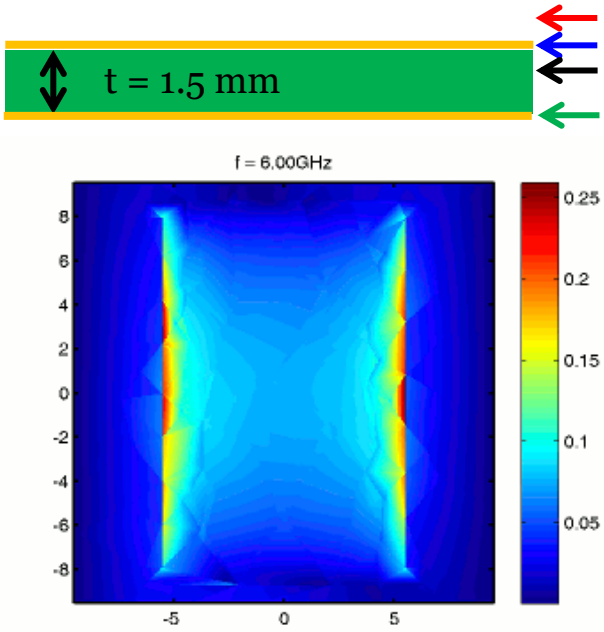

Maximum Field Enhancement Factor

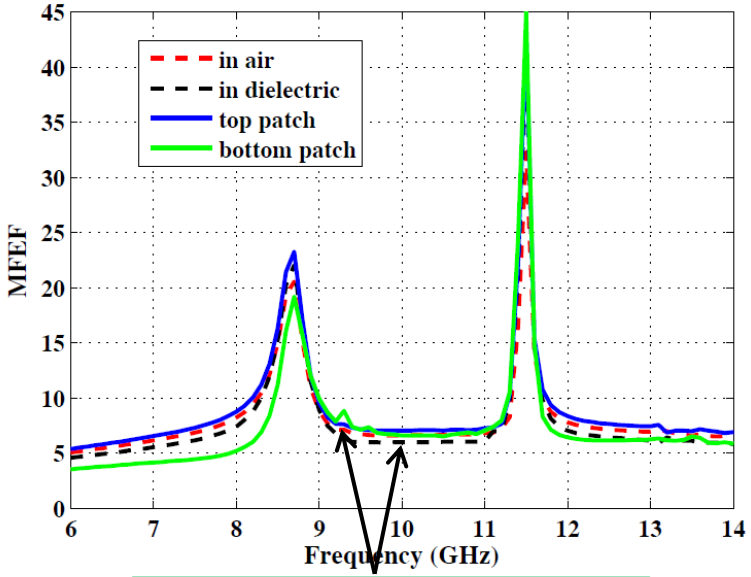

MFEF=7.6; n=-1 @ 9.22GHz
MFEF=7.0; n=0 @ 9.98GHz

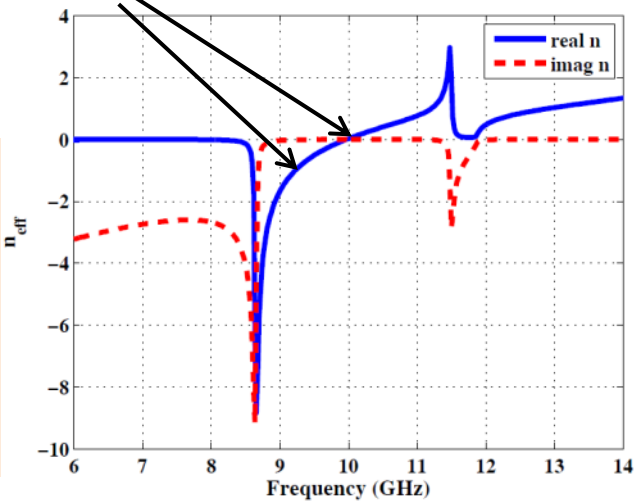

- Reduced overall field enhancement with optimized NIM design in the negative and zero index bands.
- At NIM band (n=-1), the MFEF reduced from 18 to 7.6 comparing to the previous NIM design with SRRs.
- At ZIM band (n=0), MFEF reduces from 11.5 to 7.0.

Zero- or Low-Index Metamaterial for High-power RF Applications

Quadbeam Lens with ZIM/LIM Metamaterial

The impedance and pattern bandwidths of the feed dipole were increased by adding the lens.

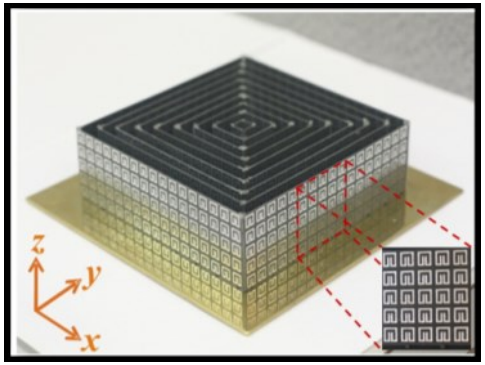

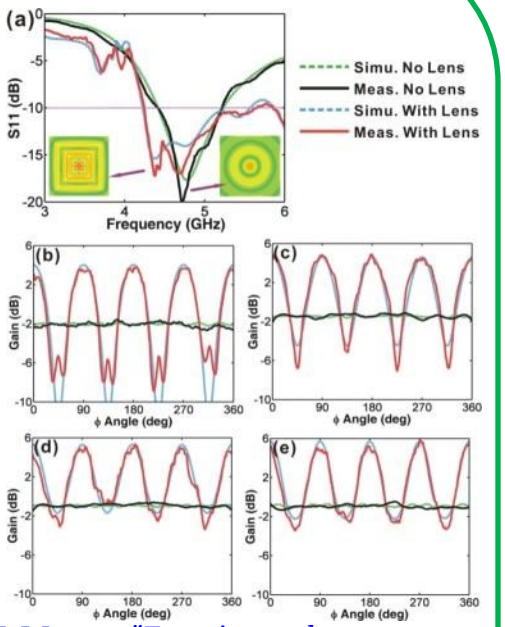

Z. H. Jiang, M. D. Gregory, and D. H. Werner, "Experimental Demonstration of a Broadband Transformation Optics Lens for Highly Directive Multibeam Emission," Phys. Rev. B, 84, 165111 (2011).

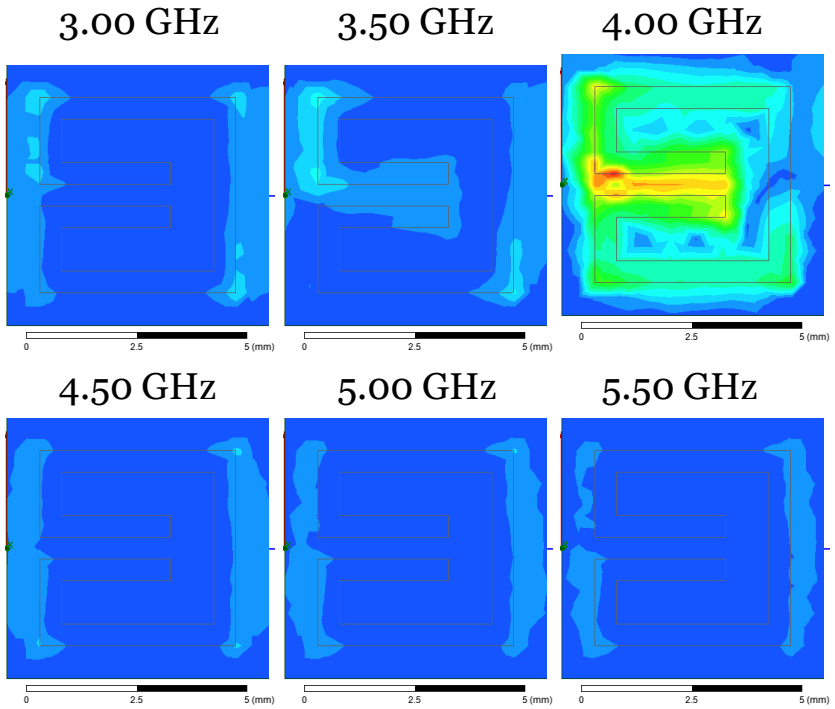

- Near-zero index metamaterials can be used to implement lenses for directive radiation.
- Full-wave simulations reveal that the field intensity can be reduced by operating away from resonance, such as in the near-zero index band, suitable for HPM applications.

Maximum Field Enhancement Factor

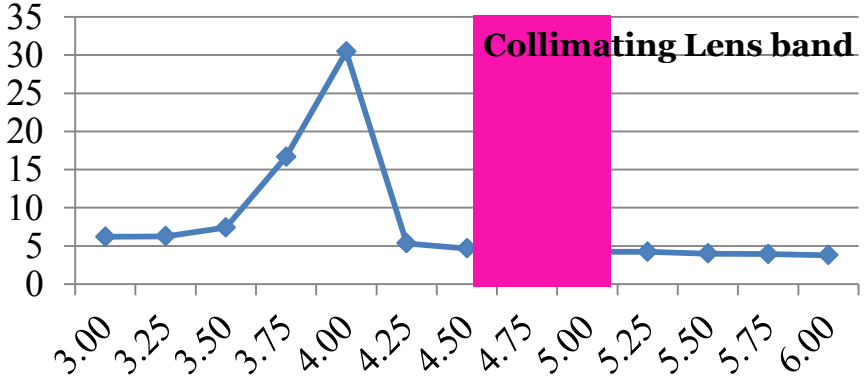

Artificial Magnetic Conductors

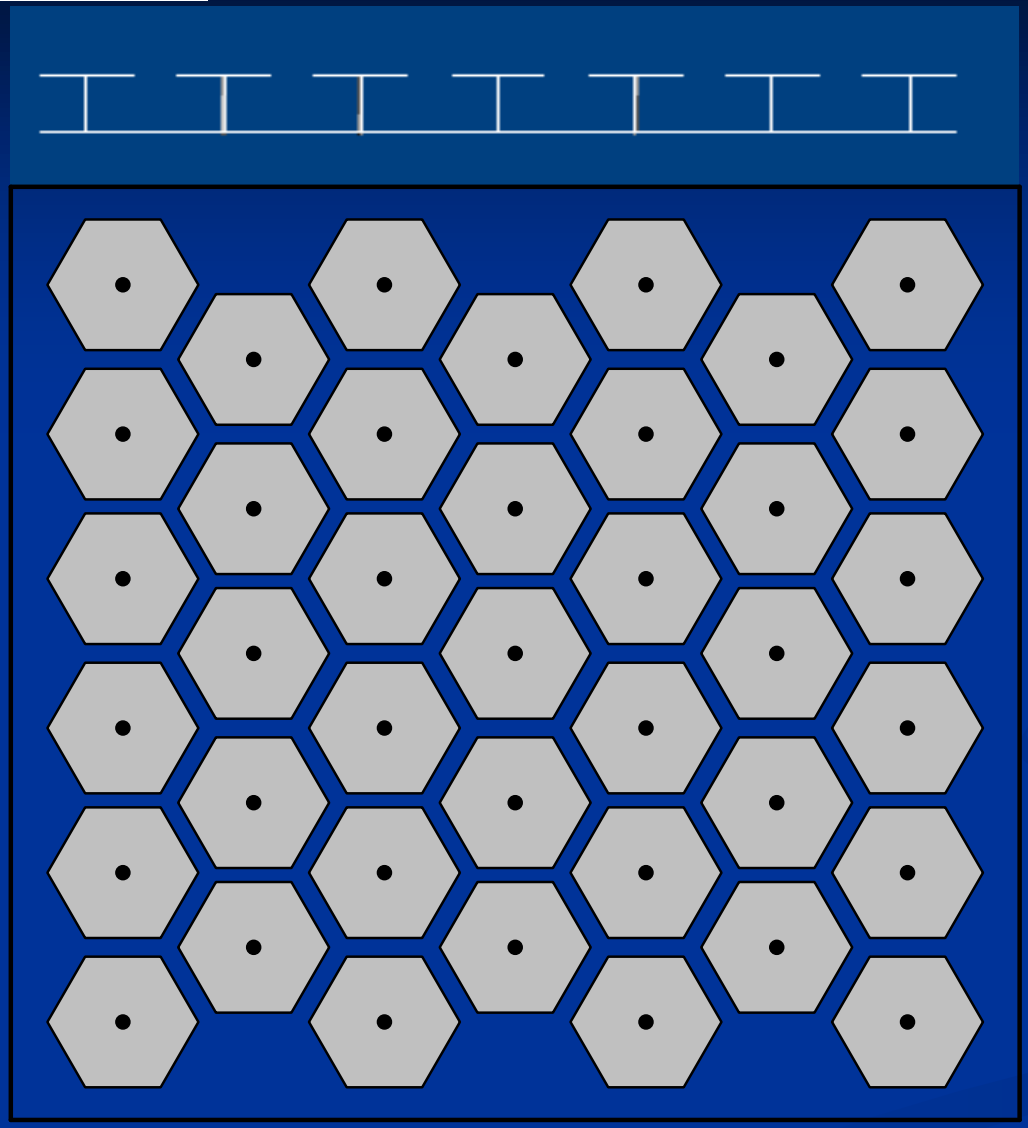

Cross section of a Sievenpiper's high-impedance surface

Top view of the Sievenpiper's high-impedance surface

Properties:

- All metallic, two layered, connected with vias.
- High-impedance surface suppresses surface waves at the forbidden frequency range

Sheet impedance

$$Z = \frac{j\omega L}{1-\omega^2 LC} \qquad \omega_0 = \frac{1}{\sqrt{LC}}$$

D. Sievenpiper, L. Zhang, Romulo F. Jimenez Broas, N. G. Alexopolous and Eli Yablonovitch, "High-Impedance Electromagnetic Surfaces with a Forbidden Frequency Band," *IEEE Transactions on Microwave Theory and Techniques*, Vol. 47, No. 11, pp. 2059 – 2074, Nov. 1999.

Artificial Magnetic Conductors

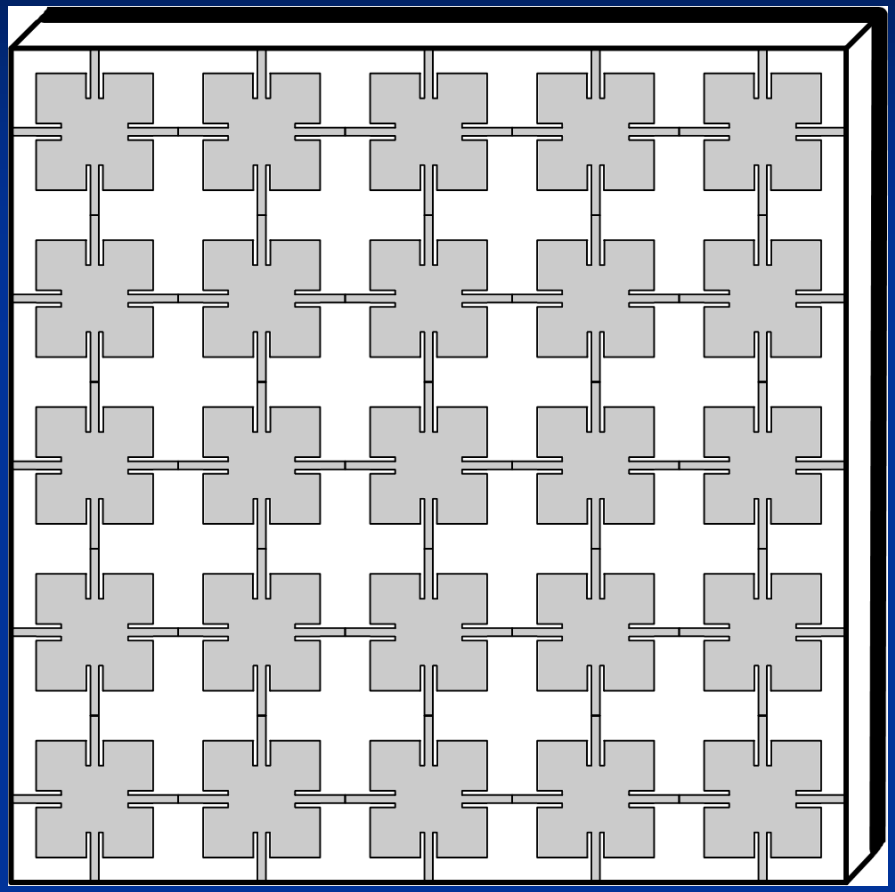

Top view of a Itoh's planar EBG surface

Properties:

- Metallo-dielectric.
- Doubly periodic Frequency Selective Surface on top of a dielectric backed by a conducting ground plane.
- If optimized; multiband (fractal), and magnetically loaded designs possible

K-P. Ma, K. Hirose, F-R. Yang, Y. Qian, and T. Itoh, "Realisation of magnetic conducting surface using novel photonic bandgab structure," *IEE Electronics Letters*, Vol. 34, No. 21, pp. 2041-2042, 15th October 1998.

Artificial Magnetic Conductors

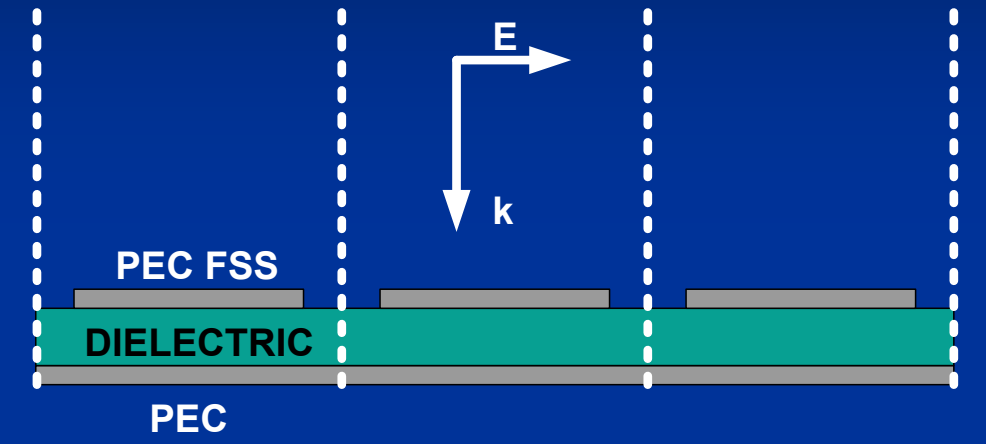

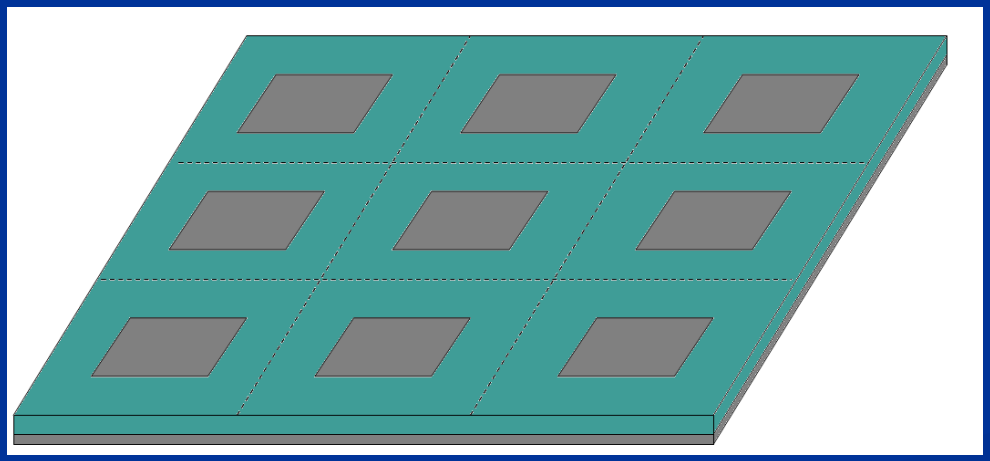

Three unitcells by three unitcells view

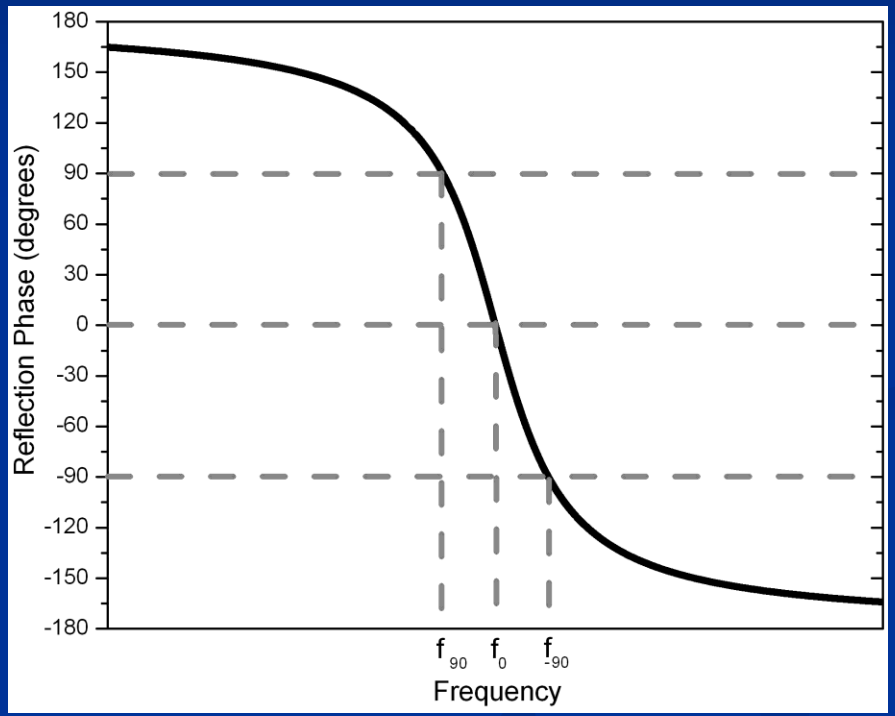

Periodic FE-BI Analysis

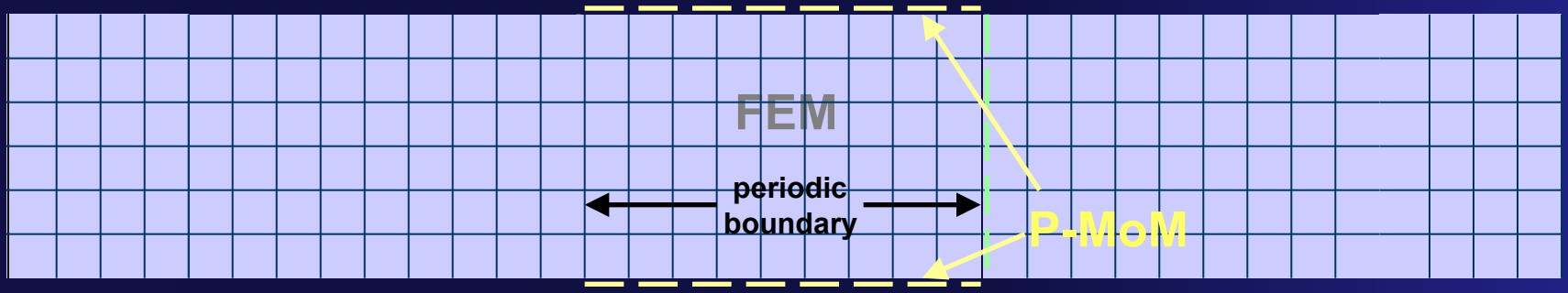

- Periodic BC → Simulate one unit cell
- Interior region: Periodic Finite Element Method (P-FEM)

$$F(E_{\text{ad}}, E) = \iiint_V \left[\frac{1}{\mu_r} (\nabla \times E_{\text{ad}}) \cdot (\nabla \times E) - k_0^2 \varepsilon_r E_{\text{ad}} \cdot E \right] dv + jk_0 Z_0 \iint_S E_{\text{ad}} \cdot (H \times n) ds$$

- Top & bottom boundary: Periodic Method of Moments (P-MoM)

$$H = -2j \frac{1}{Z_0} \left[\iint_S G_p(r, r_s)(E \times n) ds + \frac{1}{k_0^2} \nabla \iint_S G_p(r, r_s) \nabla_s \cdot (E \times n) ds \right] + H^{\text{inc}}$$

- Accelerated computation for $G_p(r, r_s)$ using Ewald transformation

PENNSTATE

GA Design Approach

Haupt and Werner (2007)

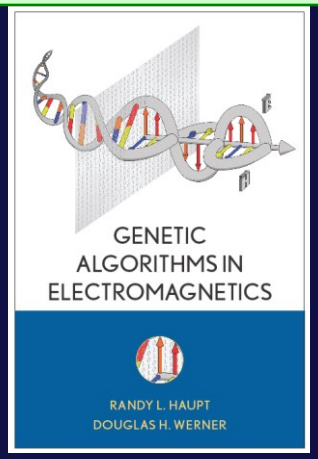

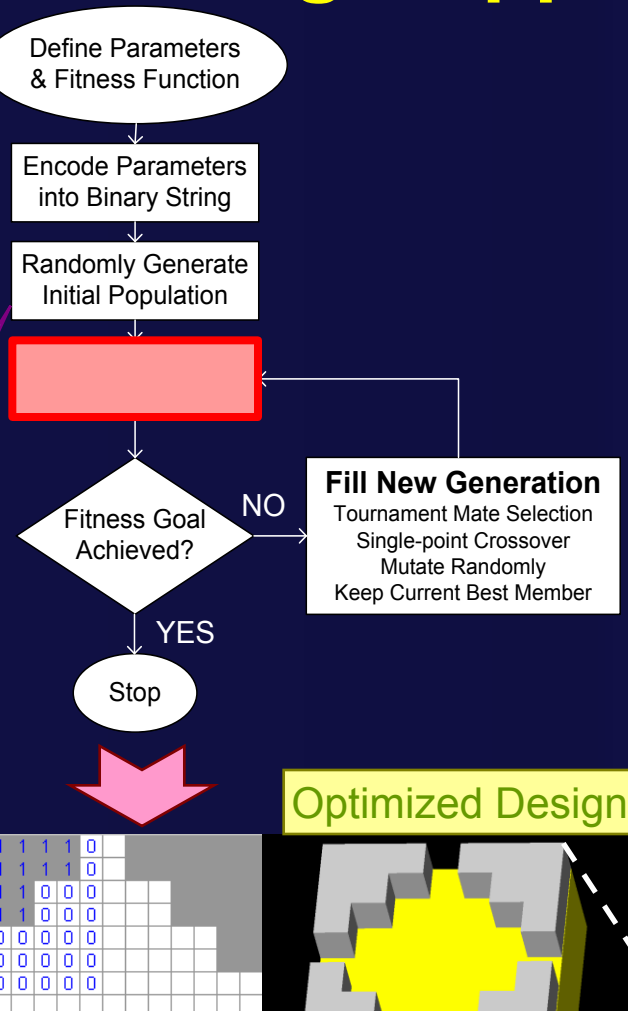

Characterization

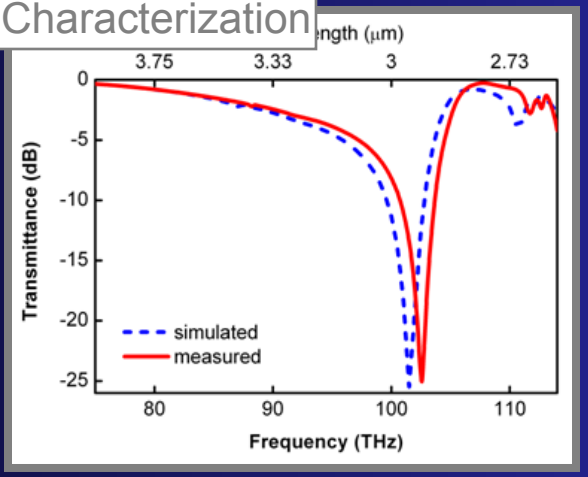

Fabrication

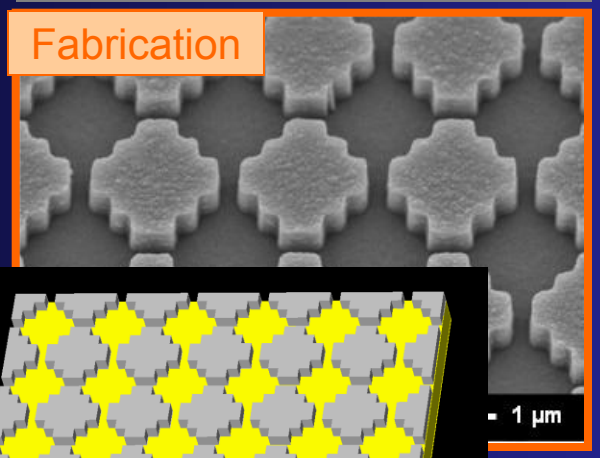

Optimized Design

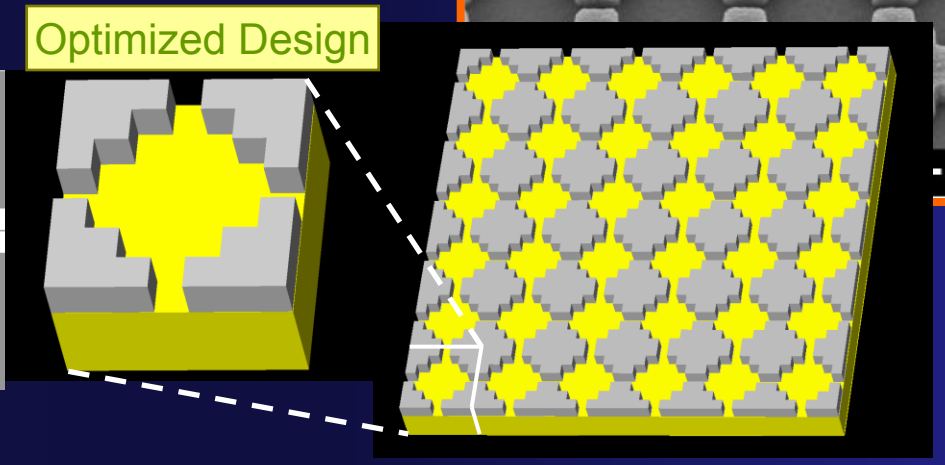

GA EBG Synthesis

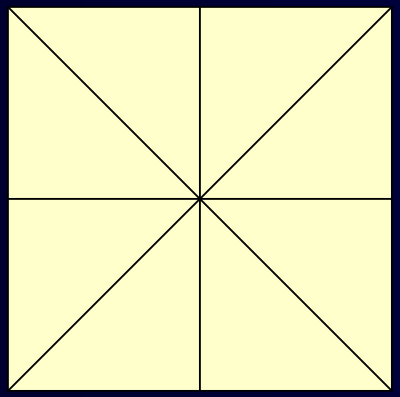

8-Fold Symmetry

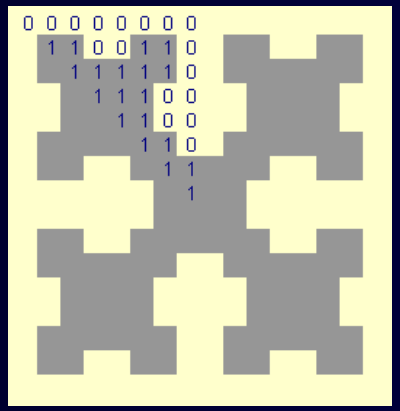

Cell Size

- **Implementation of GA**
  - **8-fold symmetry** applied to metal screen pattern to achieve polarization insensitivity
  - Cell size and other EBG parameters are encoded in the chromosome
  - Each sample is evaluated for fitness against the ideal frequency response

$$Cost = \sum_{freqs} \{\varphi_R - 0.0\}^2$$

$$Cost = \sum_{freqs} \{\varphi_R - 0.0\}^2 + \{\max(|E|) - 0.0\}^2$$

Fitness Function

FSS Cell Geometry Applying 8-Fold Symmetry | Cell Size | Other Parameters
00000000|1100110|111110|11100|1100|110|11|1 | 01101110 | ...

Single-Band AMC Optimization

Design Goal: AMC Condition at 1.25 GHz

$$Cost = \sum_{freqs} \{\varphi_R - 0.0\}^2$$

$$freqs = \{1.25\ GHz\}$$

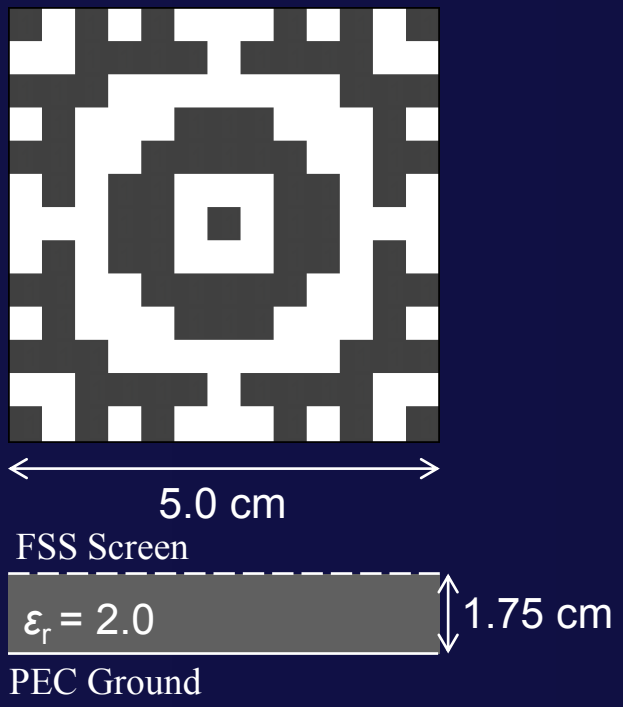

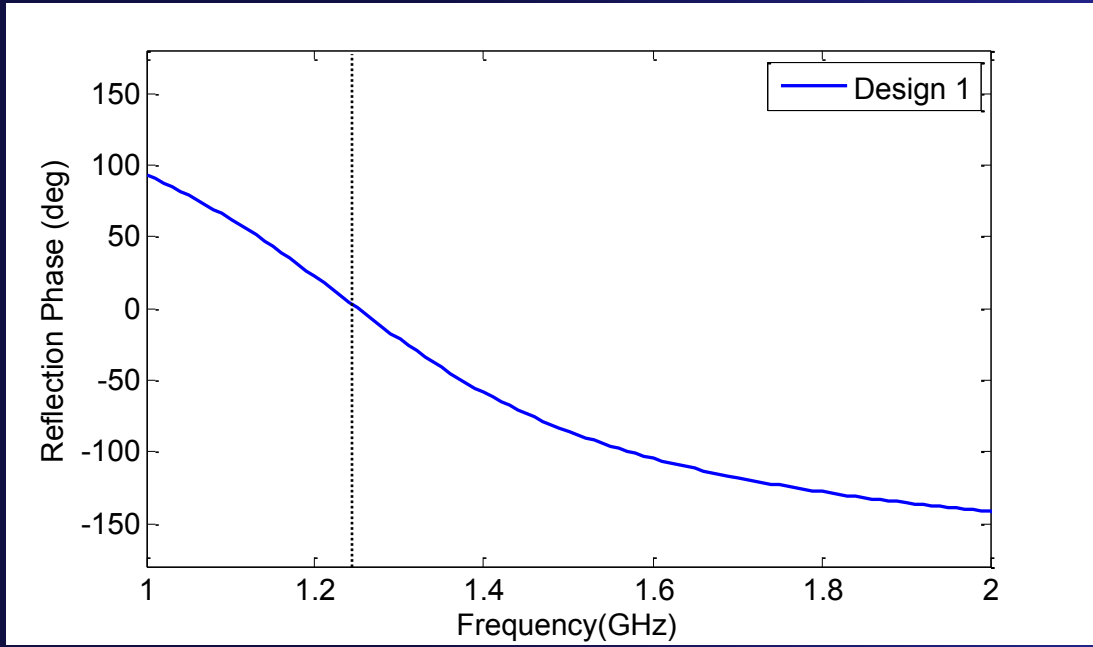

Single-Band AMC Field Enhancement

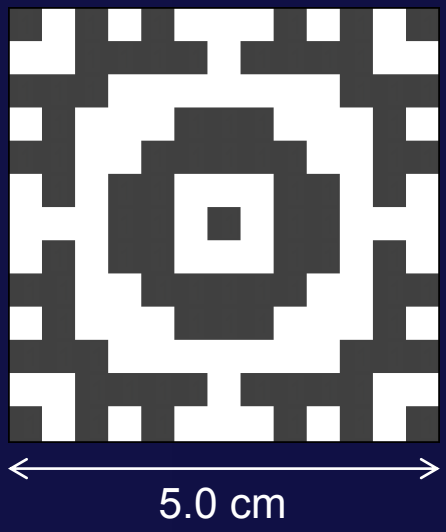

|E| Enhancement @ 1.25 GHz

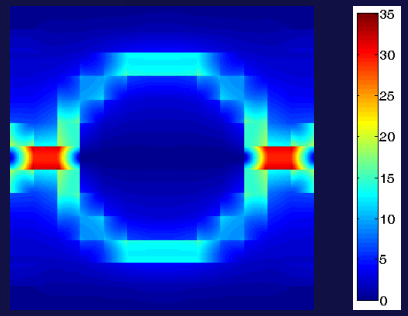

Peak MFEF of 34.7 @ 1.25 GHz.

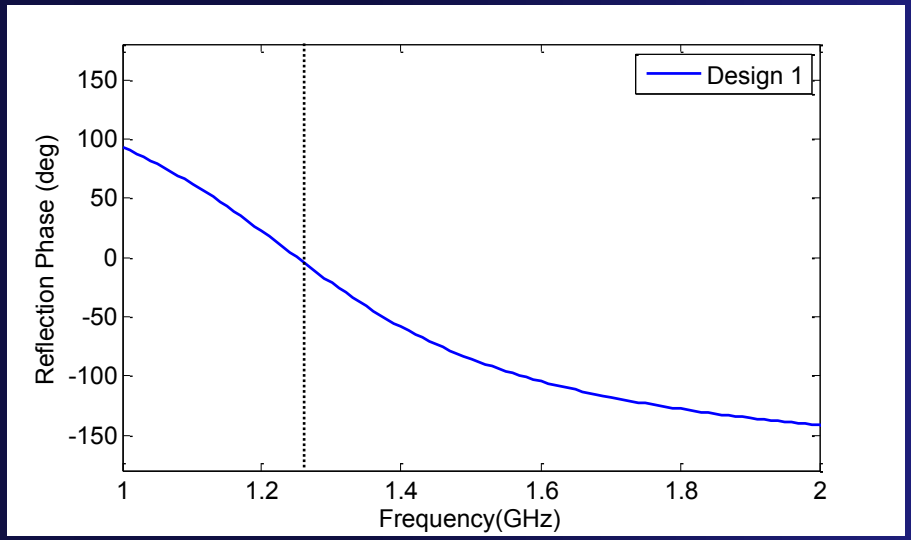

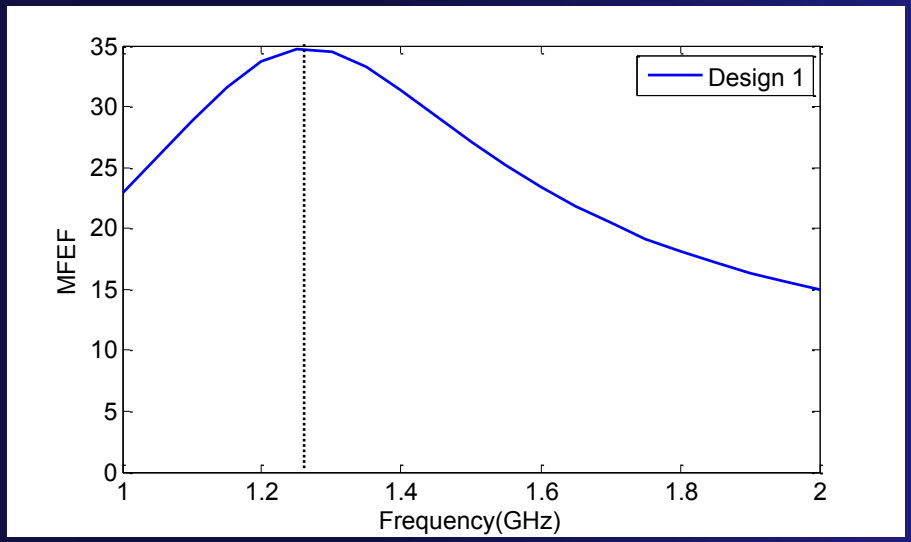

Single-Band AMC With Suppressed MFEF

Design Goal: AMC Condition at 1.25 GHz

$$Cost = \sum_{freqs} \{\varphi_R - 0.0\}^2 + \{\max(|E|) - 0.0\}^2$$

$$freqs = \{1.25\ GHz\}$$

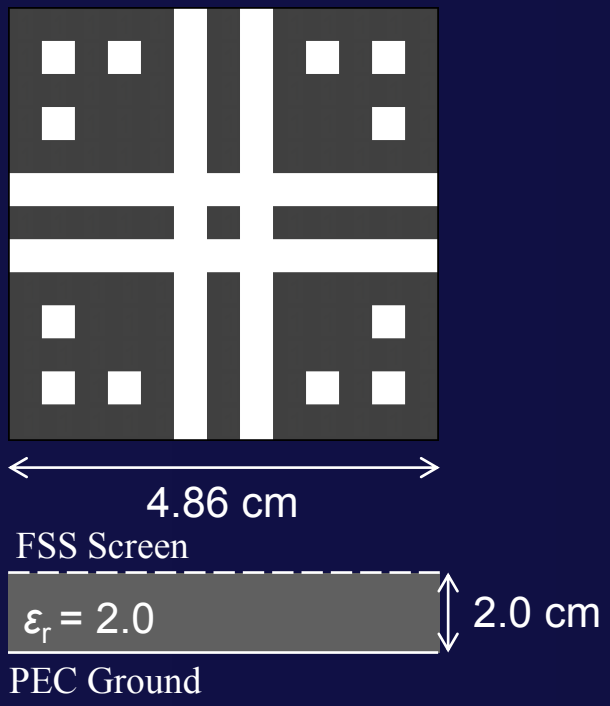

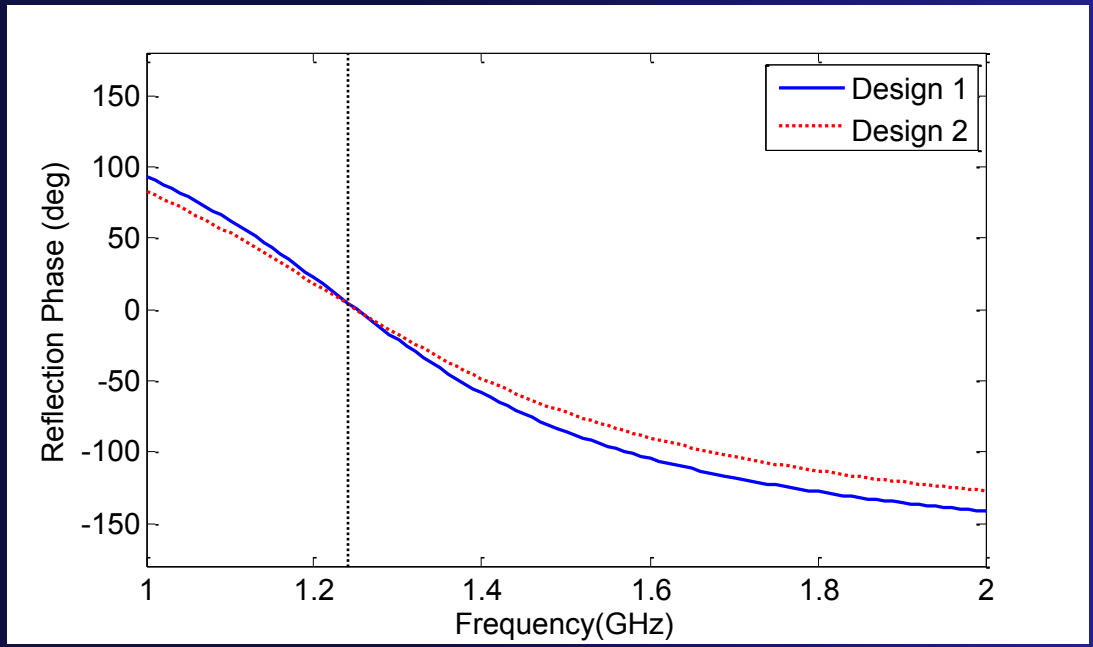

Single-Band AMC MFEF Comparison

Peak MFEF @ 1.25 GHz Reduced from 34.7 to 14.3

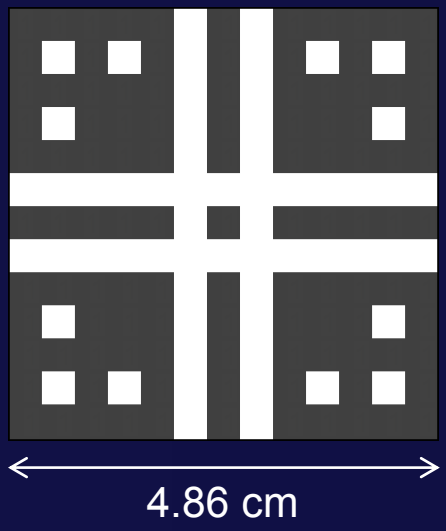

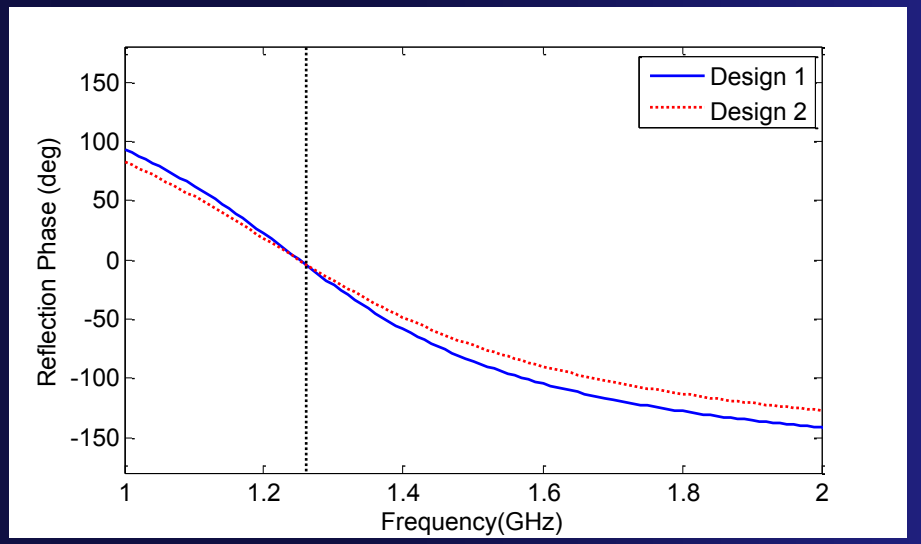

|E| Enhancement @ 1.25 GHz

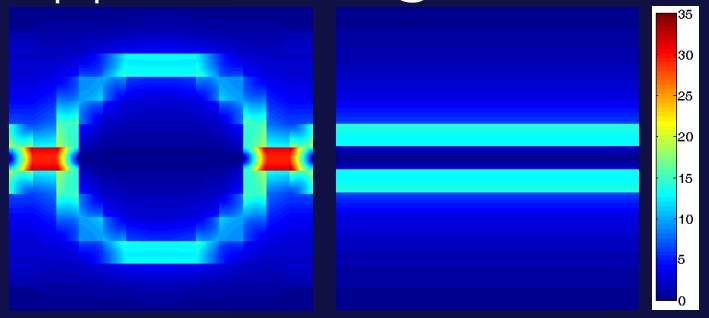

Design 1 Design 2

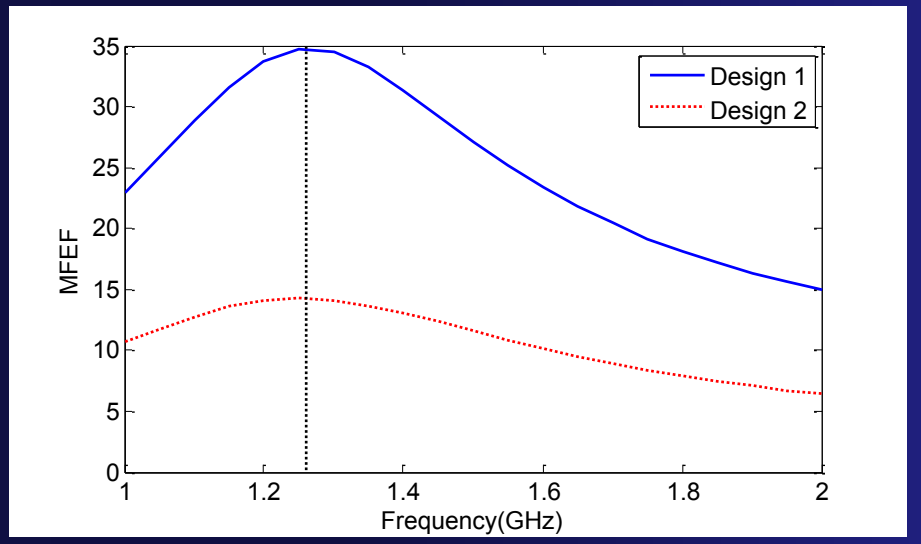

Dual-Band AMC Optimization

Design Goal: AMC Condition at 1.25 GHz and 1.75 GHz

$$Cost = \sum_{freqs} \{\varphi_R - 0.0\}^2$$

$$freqs = \{1.25\ GHz, 1.75\ GHz\}$$

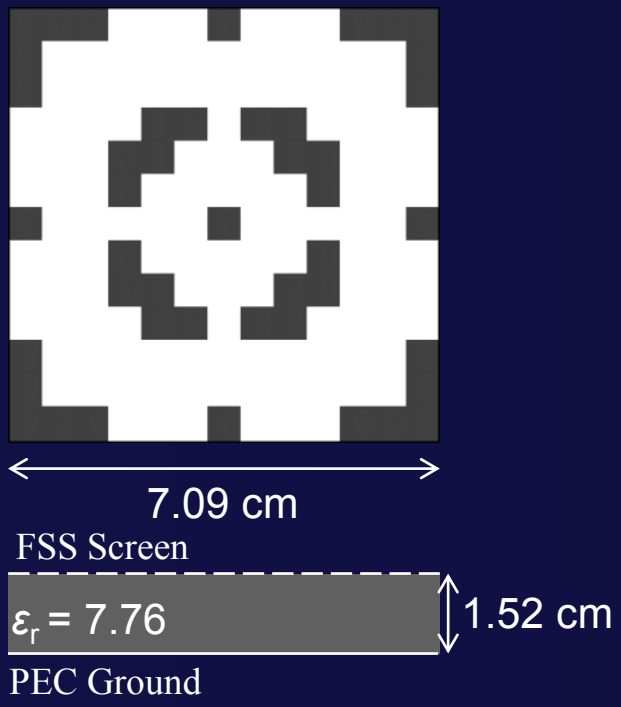

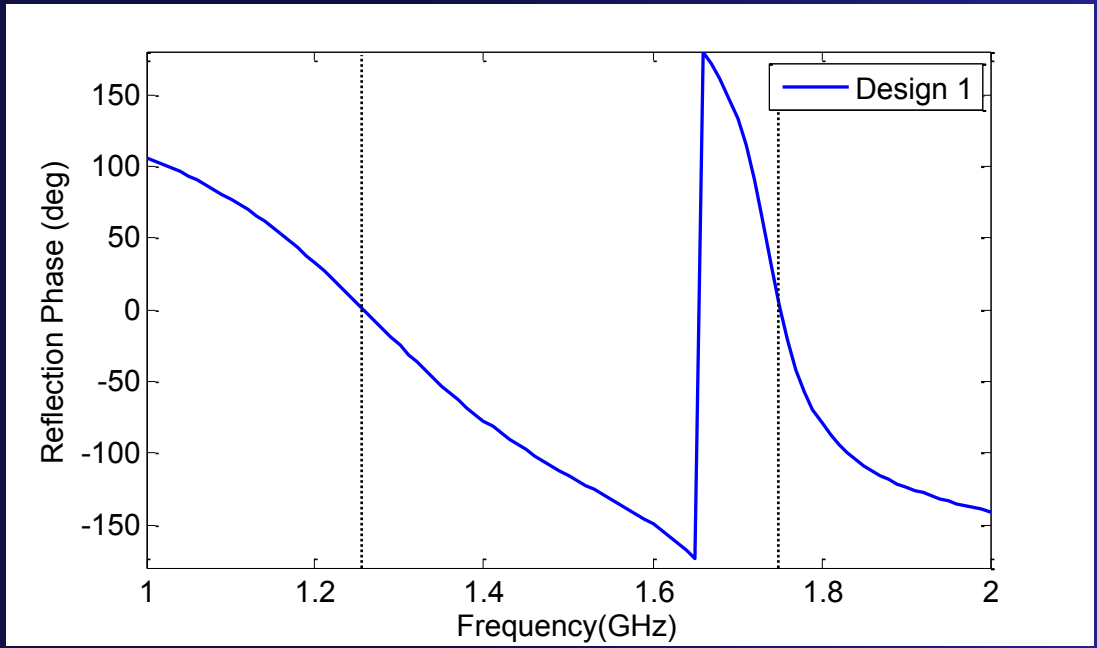

Dual-Band AMC Field Enhancement

Peak MFEF of 31.0 @ 1.75 GHz.

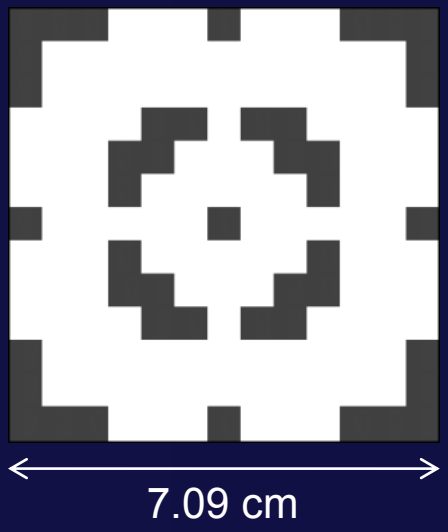

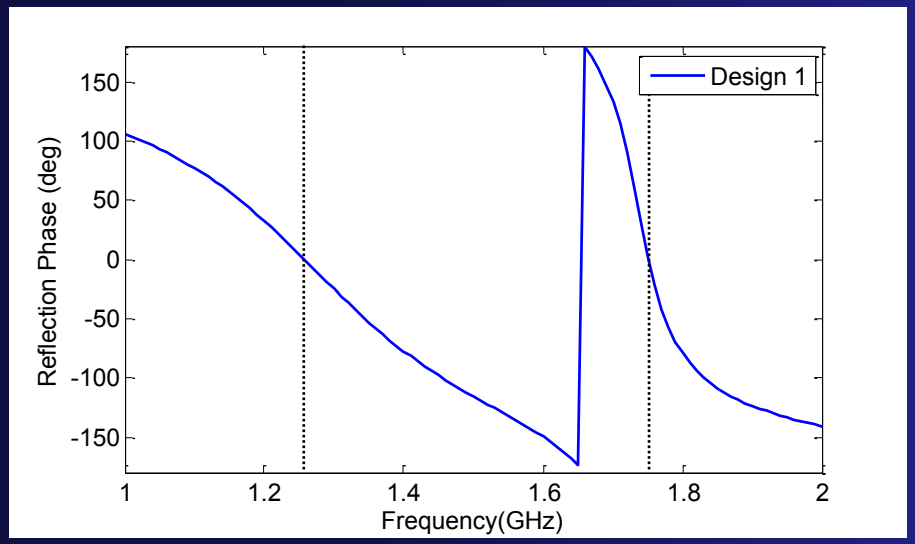

|E| Enhancement

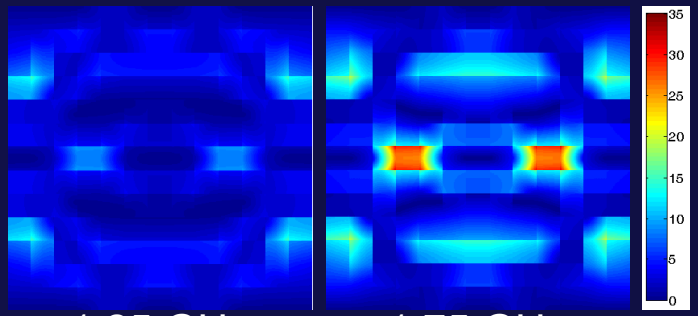

1.25 GHz 1.75 GHz

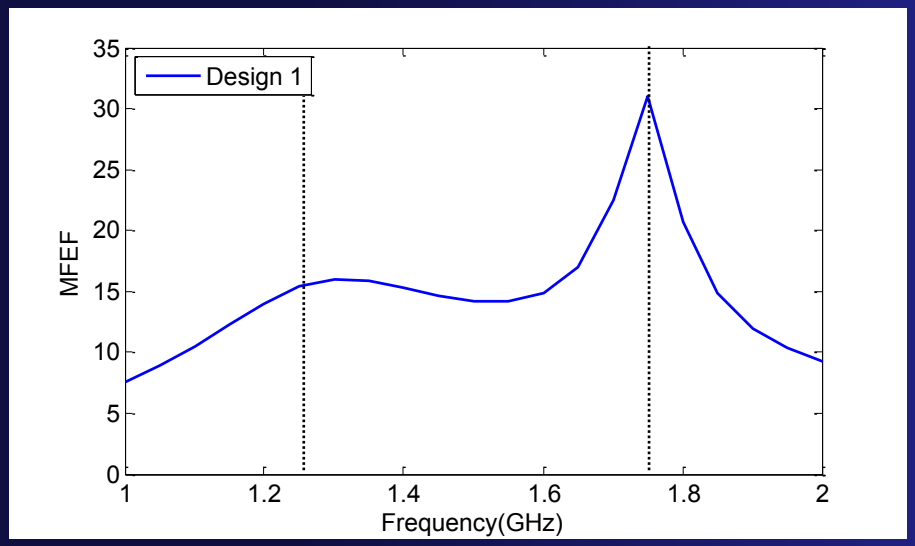

Dual-Band AMC With Suppressed MFEF

Design Goal: AMC Condition at 1.25 GHz and 1.75 GHz

$$Cost = \sum_{freqs} \{\varphi_R - 0.0\}^2 + \{\max(|E|) - 0.0\}^2$$

$$freqs = \{1.25\ GHz, 1.75\ GHz\}$$

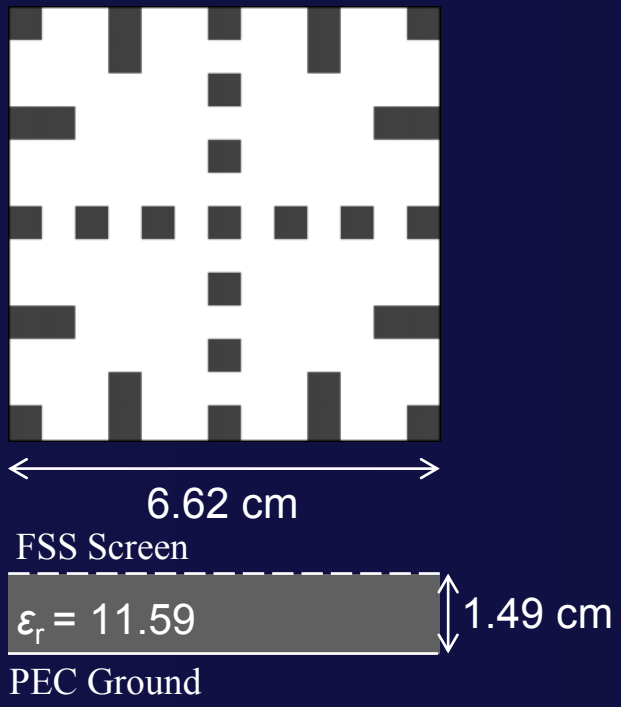

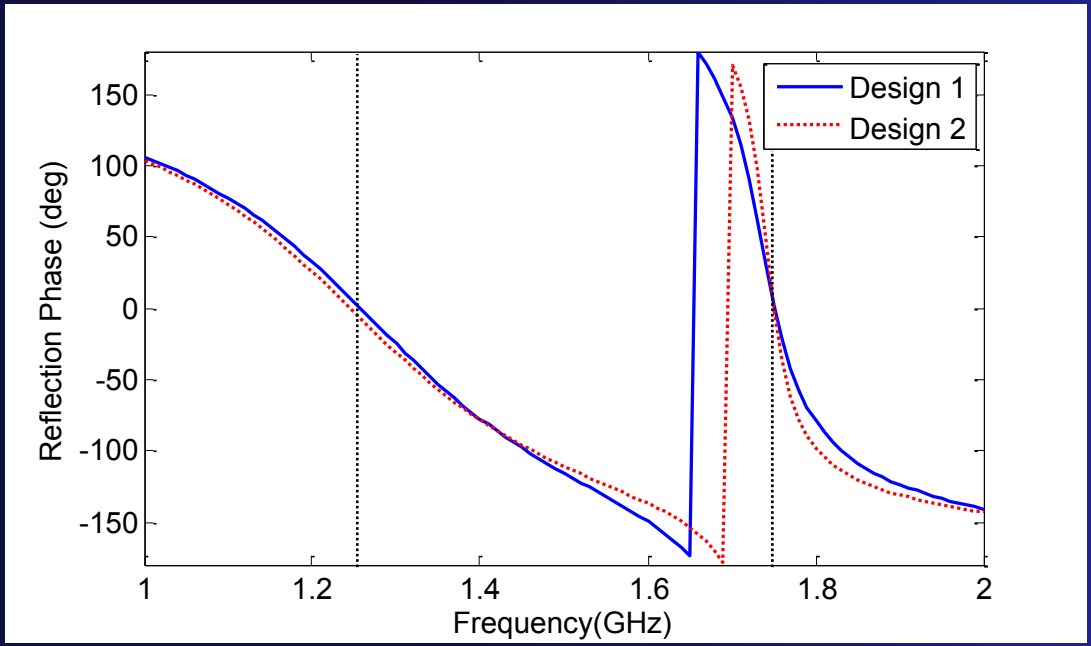

Dual-Band AMC MFEF Comparison

Peak MFEF @ 1.75 GHz Reduced from 31.0 to 15.8

Design 1 Design 2

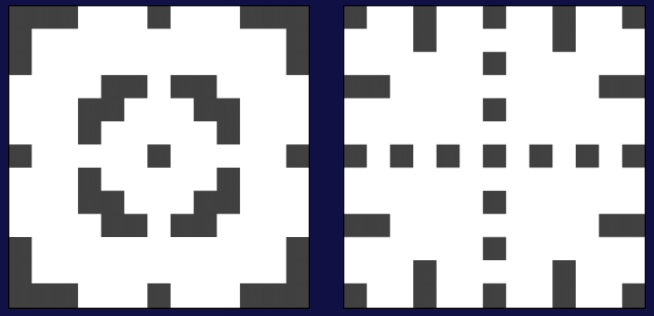

|E| Enhancement @ 1.25 GHz

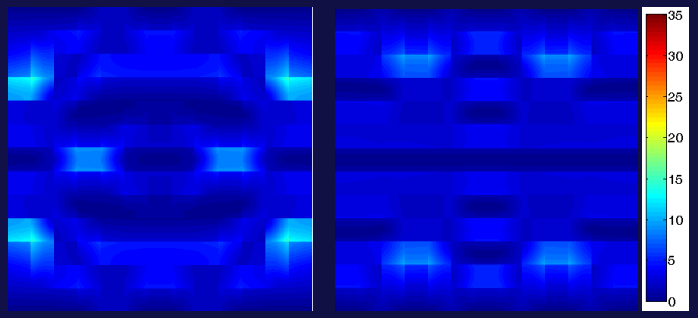

|E| Enhancement @ 1.75 GHz

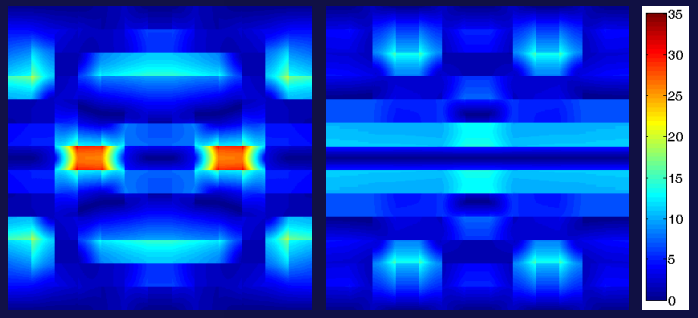

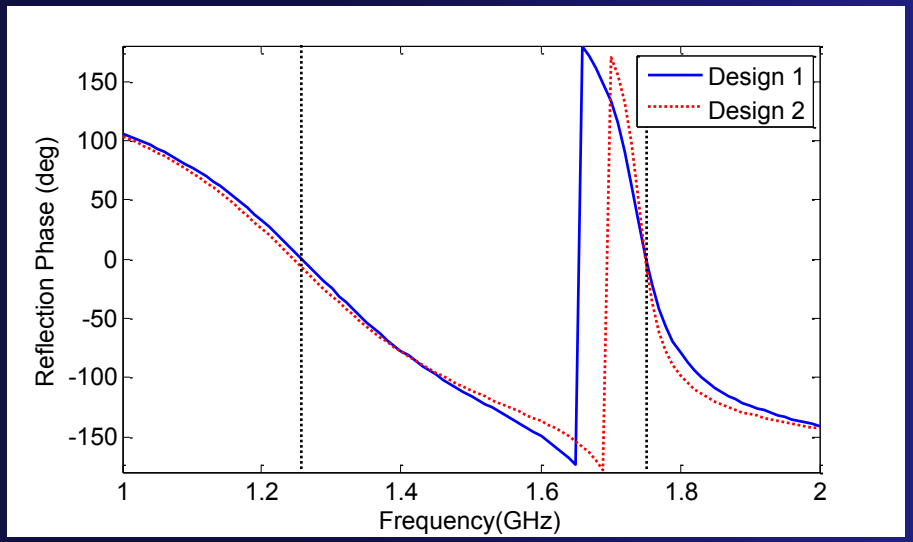

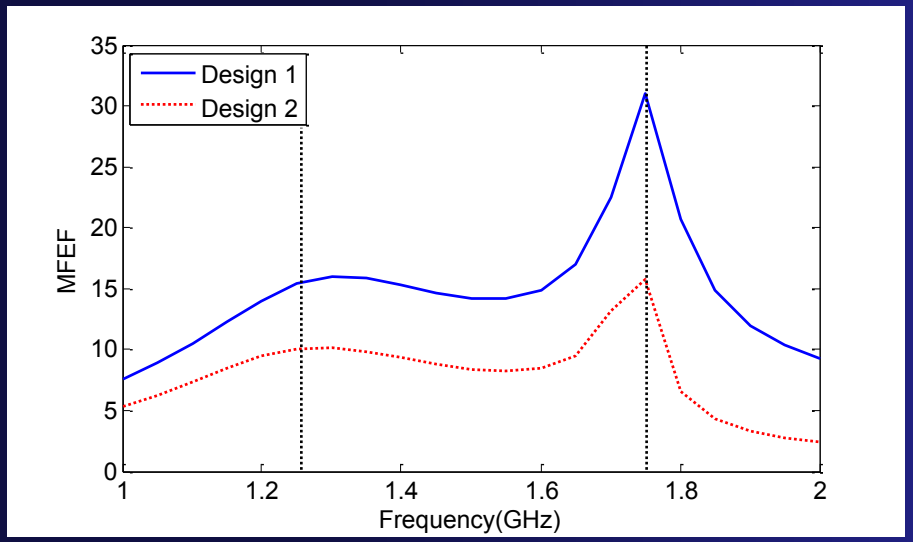

PENNSTATE

Summary

- Many metamaterial types rely on resonant behaviors that produce high fields within their structures.
- However, if a metamaterial can operate away from resonance (*e.g.*, low-index or zero-index metamaterials), it can be well-suited for HPM applications.
- Artificial Magnetic Conducting surfaces often exhibit high field enhancement at resonance with unoptomized MFEFs over 30.
- Genetic algorithm optimization was successfully employed to design single- and dual-band AMC surfaces with 50% reduced MFEF for HPM applications.